Communications

Comparison of Modeled and Measured Second Azimuthal Harmonics of Ocean Surface Brightness Temperatures

Min Zhang and Joel T. Johnson

***Abstract*—Second azimuthal harmonics of ocean surface brightness temperatures predicted by the second order small slope approximation (SSA) are compared to an empirical model based on WindRAD experiments performed by the Jet Propulsion Laboratory (JPL), Pasadena, CA. SSA predictions are illustrated for three differing models of the ocean surface directional spectrum, and results as a function of wind speed are shown to be in reasonable agreement with the WindRAD model at 19.35 and 37 GHz and at polar observation angles of 45°, 55°, and 65°. None of the three spectral models, however, completely matches all the trends of the empirical data. A slight modification to one of the spectra is demonstrated to yield an improved agreement.**

I. Introduction

Interest in polarimetric microwave radiometry for remote sensing of oceanwind speed and direction has been increasing in recent years [1]–[5]. Several experimental campaigns have been conducted, and at present, sufficient empirical evidence of wind vector retrievals exists to motivate inclusion of a polarimetric radiometer on the NPOESS generation of satellites [6]. Wind direction retrievals are possible due to the azimuthal asymmetry of a wind driven ocean surface, which can produce azimuthally varying brightness temperatures in all four modified Stokes mission parameters. These four modified Stokes parameters are labeled T_{Bh}, T_{Bv}, T_U, and T_V in this paper, respectively, where the former two quantities refer to brightness temperatures in horizontal or vertical polarizations, and the latter two quantities refer to the real and imaginary parts of the correlations between horizontally and linearly polarized fields, as described in [7]. A convenient expansion of sea surface brightness temperatures into a series of azimuthal harmonics can be made, as

$$\begin{bmatrix} T_{Bh} \\ T_{Bv} \\ T_U \\ T_V \end{bmatrix} \approx \begin{bmatrix} T_{Bh}^{(0)} + T_{Bh}^{(1)} \cos\phi_i + T_{Bh}^{(2)} \cos 2\phi_i \\ T_{Bv}^{(0)} + T_{Bv}^{(1)} \cos\phi_i + T_{Bv}^{(2)} \cos 2\phi_i \\ T_U^{(1)} \sin\phi_i + T_U^{(2)} \sin 2\phi_i \\ T_V^{(1)} \sin\phi_i + T_V^{(2)} \sin 2\phi_i \end{bmatrix} \tag{1}$$

where ϕ_i denotes the azimuth angle between the radiometer look direction and wind direction. The azimuthal harmonic coefficients $T_\gamma^{(i)}$ in the above equation remain functions of the radiometer polar observation angle, the frequency of observation, the relative permittivity of sea water, and the statistical properties of the surface and can also contain contributions from the presence of sea foam and direct and reflected atmospheric emissions.

Several modeling studies of thermal emission from sea surface shave also been performed [7]–[13] and used to explain some of the physical properties of ocean surface polarimetric brightness temperatures. In all such models, a description of the statistics of the sea surface profile is required to obtain predictions, with differing models emphasizing differing statistical information. One such model, based on a second order small slope approximation (SSA) [7], [10], requires knowledge of the ocean surface directional spectrum in order to predict both zeroth and second brightness temperature azimuthal harmonics. Prediction of first azimuthal harmonics (the "up/down" wind asymmetry) requires a third order SSA theory and knowledge of the surface bispectrum and has only been considered in limited cases [11], [14]. At present, relatively few validations of the second order SSA theory have been performed through comparison with measured data. Clearly, the model used for the ocean surface directional spectrum can have a significant influence [13].

In this paper, a more detailed study of the second order SSA theory is illustrated by comparing model predictions of second emission azimuthal harmonics with an empirical model derived from WindRAD experiments at 19.35 and 37 GHz performed by the Jet Propulsion Laboratory (JPL), Pasadena, CA, between 1994 and 1996 [15]. SSA results using three models for the ocean surface directional spectrum are compared to assess their performance, and a slight modification in one of the spectra is demonstrated to yield improved agreement with empirical data. The SSA theory and the directional spectral models used are briefly described in the next section, and the WindRAD empirical model reviewed in Section III. Data comparisons are illustrated in Section IV, and conclusions reported in Section V.

II. SSA and Directional Spectrum Models

The SSA for emission from a rough surface (shown to be identical to the small perturbation method for emission calculations in [10]) involves an expansion of rough surface emission contributions into a series in surface slope. The zeroth order term reproduces emission from a flat surface profile, the first order term identically vanishes, and the second order term provides the first correction to flat surface brightnesses, as described in [13]. The second order term is expressed as an integral over the ocean surface directional spectrum multiplied by a "weighting function" that describes the relative contribution of each surface length scale to the overall emission correction. Due to the small slope nature of the theory and in contrast to a small height perturbation point of view, no distinction between "small" and "large" scale components in the ocean surface spectrum is required, allowing contributions to be obtained for all surface spectral components in a single integration. The second order correction can furthermore be separated into zeroth and second azimuthal harmonic components, so that these quantities can be evaluated separately, again as described in [13]. In this paper, the integral for SSA second order contributions is performed over length scales ranging from 0.01 mm to 10 000 m, allowing contributions from length scales much smaller than or much greater than the 1.55 cm and 8.11 mm wavelengths at 19.35 and 37 GHz to be captured. A physical temperature of 283 K is assumed for the ocean surface, and sea water relative permittivities of $27.25 + i\ 36.36$ and $12.77 + i\ 24.09$ are used at 19.35 and 37 GHz, respectively, following the model of [16]. Note model predictions capture only emission from the rough surface and neglect any contributions to emission azimuthal harmonics due to surface foam or reflected atmospheric emissions.

Three distinct models for the sea surface directional spectrum are applied in the comparison: those of Durden–Vesecky [17], the Donelan–Banner–Jahne spectrum of Apel [18], and the "Unified" spectrum [19]. The Durden–Vesecky spectrum has been previously applied in some limited comparisons of emission azimuthal harmonics

Manuscript received September 20, 1999; revised January 7, 2000. This work was supported by Office of Naval Research (ONR) Contracts N00014-97-1-0541 and N00014-00-1-0399.

The authors are with the Department of Electrical Engineering and ElectroScience Laboratory, The Ohio State University, Columbus, OH 43210 USA (e-mail: johnson@ee.eng.ohio-state.edu).

Publisher Item Identifier S 0196-2892(01)00989-5.

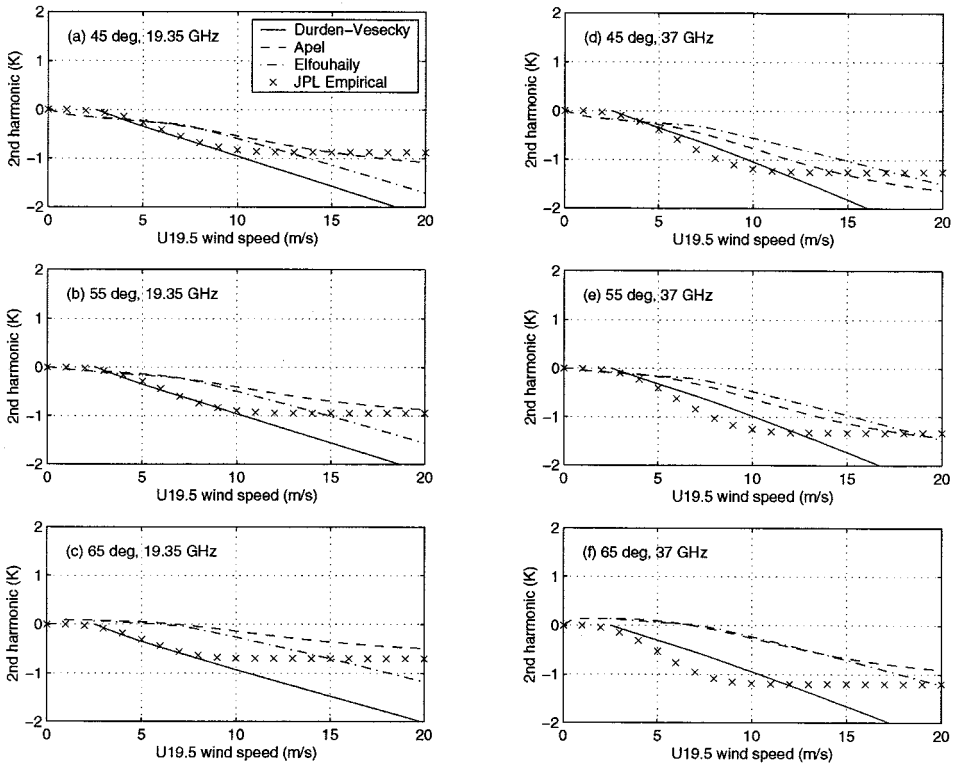

Fig. 1. Comparison of SSA and WindRAD empirical T_{Bh} second harmonics. (a) 45°, 19.35 GHz, (b) 55°, 19.35 GHz, (c) 65°, 19.35 GHz, (d) 45°, 37 GHz, (e) 55°, 37 GHz, and (f) 65°, 37 GHz.

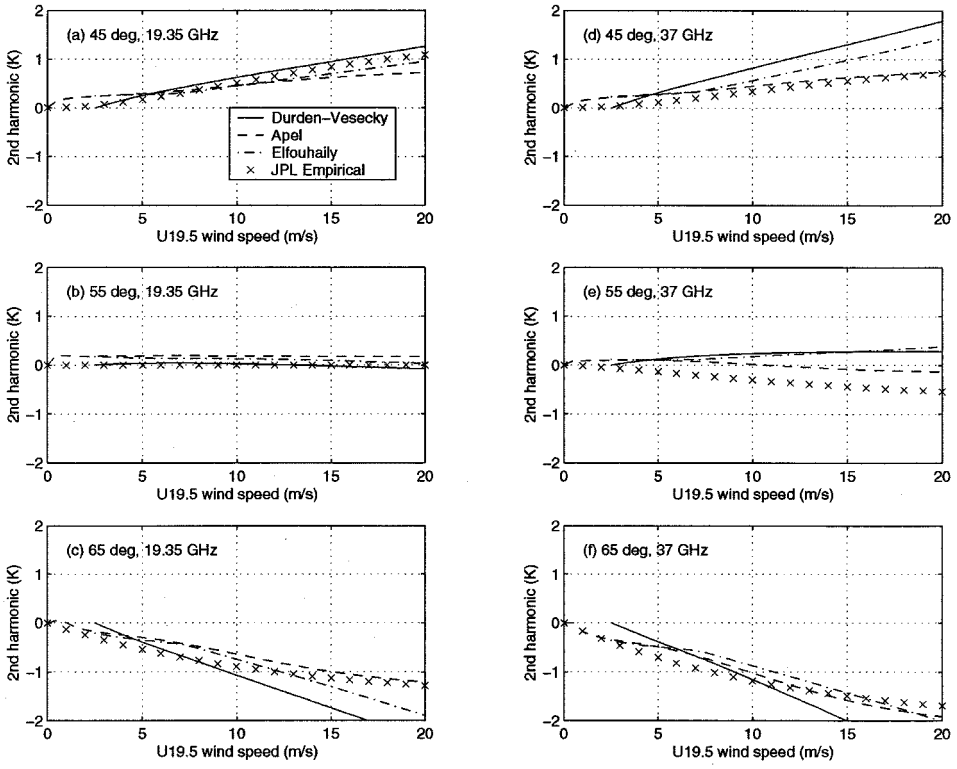

Fig. 2. Same as Fig. 1, but for T_{Bv} second harmonics.

with measured data [7], [8], and the modification of the spectral constant a_0 from 0.004 to 0.008, as suggested in [7], is also made in this paper. The Donelan–Banner–Jahne spectrum is modified in this paper to obtain proper symmetries in azimuth by using only the first quadrant of the original spectrum, which is then reflected to generate the remaining three quadrants. A factor similar to that discussed in [19] is then included to rescale the resulting spectrum so that the surface height variance remains unchanged. One modification is made

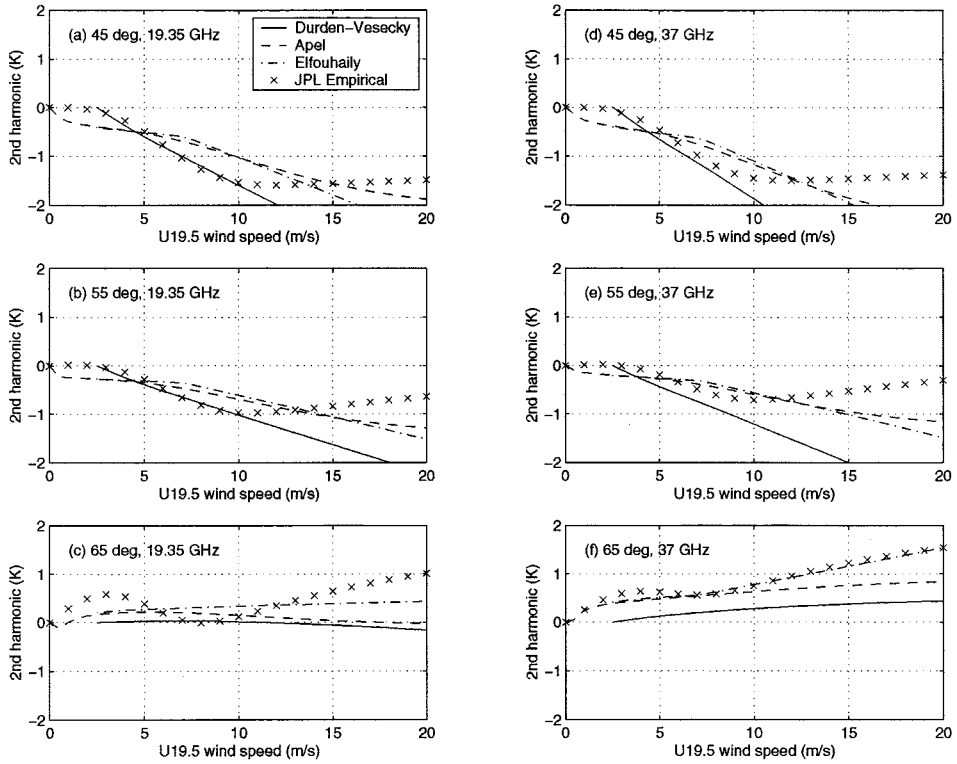

Fig. 3. Same as Fig. 1, but for T_U second harmonics.

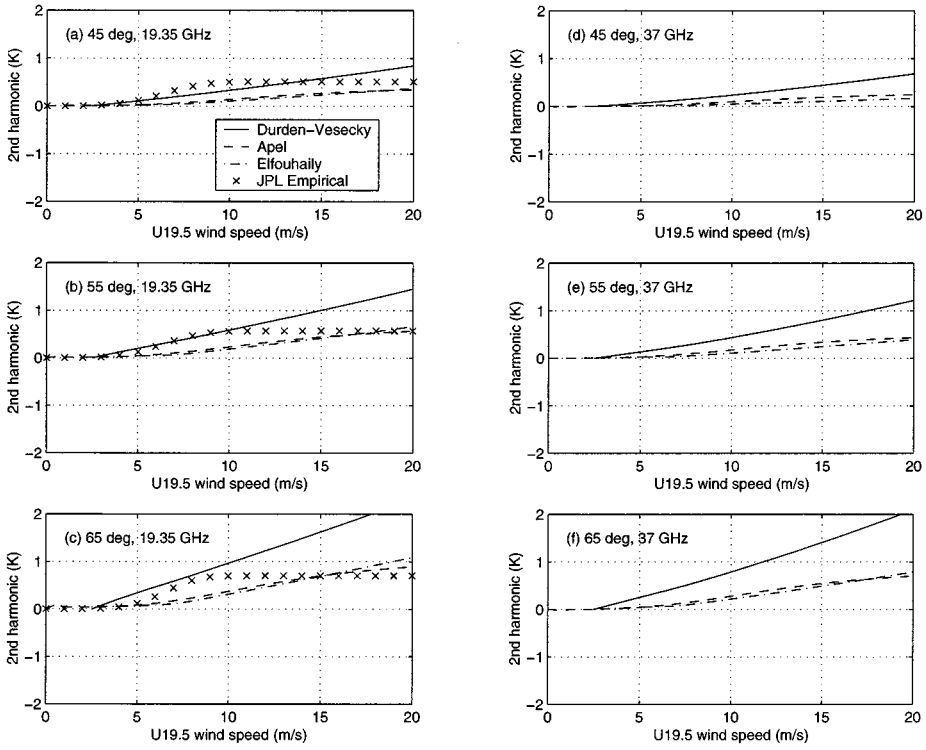

Fig. 4. Same as Fig. 1, but for T_V second harmonics. Note WindRAD model not available for 37 GHz.

to the Unified spectrum as well, based on a discussion with the authors of [19]. In this case, the term $B_l + B_h$ in the final spectrum expression of [19] is replaced with $L_{PM}[B_l/L_{PM} + B_h]$, where L_{PM} is the Pierson–Moskowitz low frequency roll-off term, to avoid excessive values for the high frequency function B_h at low frequencies. Note that the Durden–Vesecky and Unified spectra apply only for $U_{19.5}$ wind speeds greater than 2.5 m/s. The directional variations of these three spectra are quite different, with the Durden–Vesecky spectrum modeling azimuthal variations only in the capillary wave portion of the spectrum, while the Unified and Apel spectra both place azimuthal variations throughout the entire spectrum. More discussion of these differences are provided in [13] and [19].

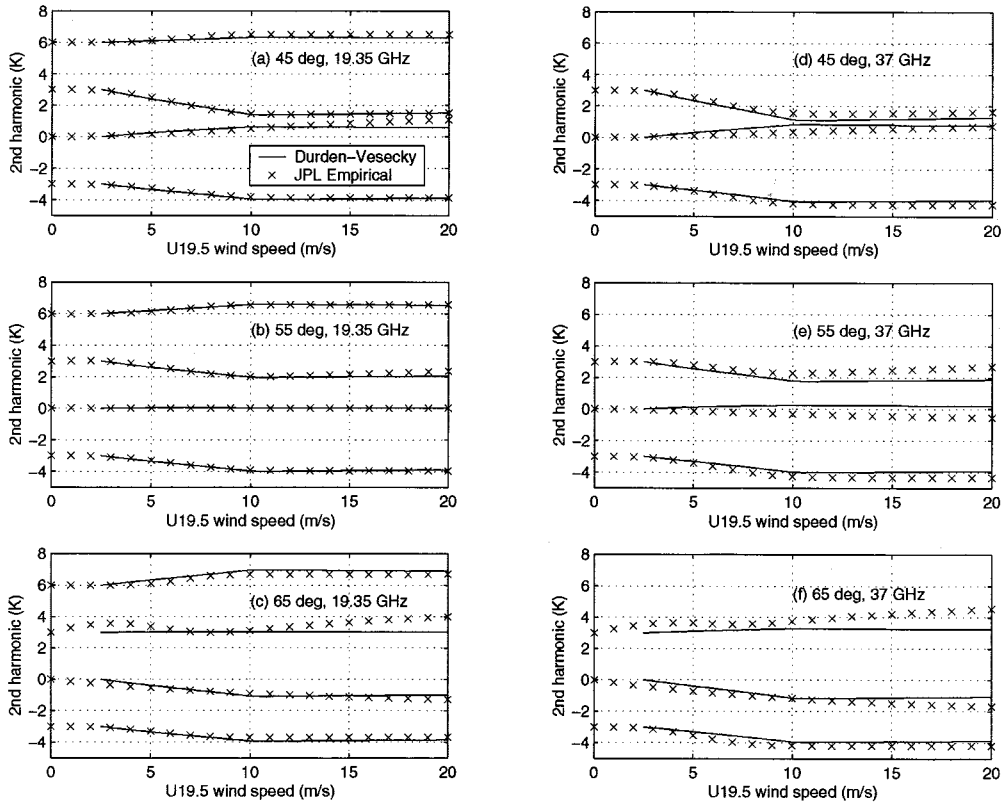

Fig. 5. Comparison of SSA using modified Durden–Vesecky spectrum with WindRAD empirical second harmonics. T_{Bh}, T_{Bv}, T_U, and T_V second harmonics are shifted by -3, 0, $+3$, and $+6$ K, respectively, to enable curves to be distinguished. (a) 45°, 19.35 GHz, (b) 55°, 19.35 GHz, (c) 65°, 19.35 GHz, (d) 45°, 37 GHz, (e) 55°, and 37 GHz (f) 65°, 37 GHz.

III. WindRAD Empirical Model

The WindRAD radiometer was operated in a series of aircraft flights by JPL between 1994 and 1996 [2], [3] and measured all four modified Stokes parameters at 19.35 GHz and the first three parameters at 37 GHz. Extensive data was acquired at polar observation angles of 45°, 55°, and 65° for varying $U_{19.5}$ wind speeds ranging from 2 to 18 m/s (measured in the experiments by the National Data Buoy Center). First order corrections to this data for variations in aircraft pitch and roll angles and for the contributions of atmospheric attenuation and emission were also developed to produce estimates of surface and foam emission contributions only. Azimuthal first and second harmonic coefficients [as described in (1)] were extracted from these data versus wind speed, and the results fit with curves of the form

$$f\left(U_{19.5}\right) = c_1\left[1 - e^{-(U_{19.5}/a_1)^{b_1}}\right] + c_2\left[1 - e^{-(U_{19.5}/a_2)^{b_2}}\right] \tag{2}$$

to create the WindRAD empirical model. The second term in the above equation is included only for third Stokes parameter fits. Coefficients c_1, c_2, a_1, a_2, b_1, and b_2 are provided in [15] for first and second azimuthal harmonics of the 19.35 and 37 GHz frequencies and for polar observation angles 45°, 55°, and 65°. Again, only a comparison of second azimuthal harmonics is considered in this paper due to the limitations of the second order SSA theory. Note an empirical model for zeroth azimuthal harmonics was not reported due to the excessive sensitivity of these quantities to atmospheric and foam effects; first and second azimuthal harmonics should be less sensitive to these contributions.

IV. Results

Figs. 1–4 illustrate the comparison of SSA results with the WindRAD empirical model for the three ocean spectral models considered. Each figure plots second harmonics of one of the four polarimetric quantities (T_{Bh}, T_{Bv}, T_U, and T_V, respectively) for the three polar observation angles and two frequencies. Note the WindRAD empirical model is not available for the 37 GHz, T_V results, so only SSA predictions are included in the corresponding plots.

In general in these results, all models predict azimuthal second harmonics on the order of 1° to 2° K, with increasing harmonic amplitudes as wind speeds increase. Agreement between the empirical and SSA models is reasonable for all three surface spectral models in the cases illustrated, and general trends of the empirical curves are reproduced in the simulations. However, the saturation that occurs in many of the WindRAD model predictions above wind speeds of approximately 10 m/s is not well captured by any of the directional spectra. When SSA predictions are continued at higher wind speeds (up to 35 m/s), a saturation in the Apel spectrum predictions is observed above 20 m/s, while the Unified and Durden–Vesecky predictions continue to increase in magnitude. It is noted that the saturation of the empirical model at wind speeds greater than 11 m/s in the T_{Bh} and T_{Bv} channels may be less reliable due to the influence of other surface and atmospheric features in these channels, as described in [15].

Predictions using the Apel and Unified spectrum models are generally observed to show more similar trends than those using the Durden–Vesecky spectrum. This result is not surprising since the Unified spectrum builds on many of the same observations as the Apel spectrum, while the Durden–Vesecky spectrum was derived independently to match ocean surface back scattering measurements. The Durden–Vesecky model appears to provide to best agreement at

19.35 GHz for low to moderate wind speeds (as has been shown in previous comparisons for this wind speed range [8]) but dramatically overestimates harmonic quantities at higher wind speeds. None of the three spectral models capture the relatively large amplitudes in 19.35 GHz, 65° T_U second harmonics at low wind speeds.

Based on the success of the Durden–Vesecky predictions for low to moderate wind speeds at 19.35 GHz, a simple modification to this spectrum is considered to obtain improved agreement at higher wind speeds. The Durden–Vesecky spectrum in the gravity-capillary region involves a function of the form

$$\frac{\left(bk\,u_*^2/g\right)^{a\log_{10}(k/2)}}{k^4} \tag{3}$$

where

k	ocean spatial frequency in rads/m;
u_*	surface friction velocity in m/s;
g	modified gravitational acceleration;
a and b	constants [17].

The spectrum is modified by replacing this function with

$$\frac{\left(bk(0.37)^2/g\right)^{a\log_{10}(k/2)}}{k^4} \tag{4}$$

for $u_* \geq 0.37$ m/s, and retaining the original form for $u_* < 0.37$ m/s. This modification is made purely to reproduce the harmonic amplitude saturation around $U_{19.5}$ wind speed 10 m/s observed in the comparisons. Such a modification appears reasonable, however, given the growth without bound that occurs as wind speeds increase in the original form.

Fig. 5 illustrates the comparisons with the modified Durden–Vesecky spectrum. In this figure, all four polarimetric quantities are illustrated in a single plot, but T_{Bh}, T_{Bv}, T_U, and T_V second harmonics are shifted by -3, 0, $+3$, and $+6$ K, respectively, to allow the curves to be distinguished. A dramatic improvement in agreement is observed for the modified spectrum, particularly at 19.35 GHz, although some differences still remain. The implication of this success is not clear, since both the sea surface directional spectrum and other emission processes may be contributors at higher wind speeds.

V. Conclusions

Results of these comparisons demonstrate that the second order SSA appears to capture many of the physical processes that produce second harmonic variations of ocean surface brightness temperatures. Differences between SSA predictions under the three ocean spectral models considered illustrate the importance of improved knowledge of the ocean surface spectrum, and in particular, its directional properties. The success of the modified Durden–Vesecky spectrum in matching the empirical model is encouraging, but several issues regarding the accuracy of this spectrum (in particular its model of the long gravity wave portion of the spectrum as azimuthally isotropic) remain [19]. Research into these issues is continuing, along with studies of the third order SSA and sea surface bispectrum for prediction of emission first azimuthal harmonics.

References

[1] M. S. Dzura, V. S. Etkin, A. S. Khrupin, M. N. Pospelov, and M. D. Raev, "Radiometers polarimeters: Principles of design and applications for sea surface microwave emission polarimetry," in *Proc. Int. Geoscience and Remote Sensing Soc. Conf. '92*, Houston, TX, 1992, pp. 1432–1434.

[2] S. H. Yueh, W. J. Wilson, F. K. Li, S. V. Nghiem, and W. B. Ricketts, "Polarimetric measurements of sea surface brightness temperatures using an aircraft K-band radiometer," *IEEE Trans. Geosci. Remote Sensing*, vol. 33, pp. 85–92, 1995.

[3] ——, "Polarimetric brightness temperatures of sea surfaces measured with aircraft K- and Ka-band radiometers," *IEEE Trans. Geosci. Remote Sensing*, vol. 35, pp. 1177–1187, 1997.

[4] V. G. Irisov and Y. G. Trokhimovski, "Observation of the ocean brightness temperature anisotropy during the coastal ocean probing experiment," in *Proc. Int. Geoscience and Remote Sensing Soc. Conf. '96*, vol. 3, Seattle, WA, 1996, pp. 1457–1459.

[5] J. R. Piepmeier, A. J. Gasiewski, M. Klein, V. Boehm, and R. C. Lum, "Ocean surface wind direction measurement by scanning polarimetric microwave radiometry," in *Proc. Int. Geoscience and Remote Sensing Soc. Conf. '98*, vol. 5, Seattle, WA, 1998, pp. 2307–2310.

[6] S. D. Gasster and G. M. Flaming, "Overview of the conical microwave imager/sounder development for the NPOESS program," in *Proc. Int. Geoscience and Remote Sensing Soc. Conf. '98*, vol. 1, Seattle, WA, 1998, pp. 268–271.

[7] S. H. Yueh, R. Kwok, F. K. Li, S. V. Nghiem, and W. J. Wilson, "Polarimetric passive remote sensing of ocean wind vectors," *Radio Sci.*, vol. 29, pp. 799–814, 1994.

[8] S. H. Yueh, "Modeling of wind direction signals in polarimetric sea surface brightness temperatures," *IEEE Trans. Geosci. Remote Sensing*, vol. 35, pp. 1400–1418, 1997.

[9] D. B. Kunkee and A. J. Gasiewski, "Simulation of passive microwave wind direction signatures over the ocean using an asymmetric-wave geometrical optics model," *Radio Sci.*, vol. 32, p. 59, 1997.

[10] V. G. Irisov, "Small-slope expansion for thermal and reflected radiation from a rough surface," *Waves Random Media*, vol. 7, pp. 1–10, 1997.

[11] ——, "Azimuthal variations of the microwave radiation from a slightly non-Gaussian sea surface," *Radio Sci.*, vol. 35, pp. 2329–2332, Sept. 1999.

[12] J. T. Johnson, R. T. Shin, L. Tsang, K. Pak, and J. A. Kong, "A numerical study of ocean polarimetric thermal emission," *IEEE Trans. Geosci. Remote Sensing*, vol. 37, pp. 8–20, Jan. 1999.

[13] J. T. Johnson and M. Zhang, "Theoretical study of the small slope approximation forocean polarimetric thermal emission," *IEEE Trans. Geosci. Remote Sensing*, vol. 37, pp. 2305–2316, Sept. 1999.

[14] J. T. Johnson and Y. Cai, "A theoretical study of sea surface up/down wind brightness temperature differences," *IEEE Trans. Geosci. Remote Sensing*, to be published.

[15] S. H. Yueh, W. J. Wilson, S. J. Dinardo, and F. K. Li, "Polarimetric microwave brightness signatures of ocean wind directions," *IEEE Trans. Geosci. Remote Sensing*, vol. 37, pp. 949–959, Mar. 1999.

[16] L. A. Klein and C. T. Swift, "An improved model for the dielectric constant of sea water at microwave frequencies," *IEEE Trans. Antennas Propagat.*, vol. AP-25, pp. 104–111, 1977.

[17] S. L. Durden and J. F. Vesecky, "A physical radar cross-section model for a wind driven sea with swell," *IEEE J. Oceanic Eng.*, vol. OE-10, pp. 445–451, 1985.

[18] J. R. Apel, "An improved model of the ocean surface wave vector spectrum and its effects on radar backscatter," *J. Geophys. Res.*, vol. 99, pp. 16 269–16 291, 1994.

[19] T. Elfouhaily, B. Chapron, K. Katsaros, and D. Vandemark, "A unified directional spectrum for long and short wind-driven waves," *J. Geophys. Res.*, vol. 102, pp. 15 780–15 796, 1997.